



Community Climate Simulations to assess avoided impacts in 1.5°C and 2°C futures

Benjamin M. Sanderson¹, Yangyang Xu², Claudia Tebaldi¹, Michael Wehner³, Brian O'Neill¹, Alexandra Jahn⁴, Angeline G. Pendergrass¹, Flavio Lehner¹, Warren G. Strand¹, Lei Lin⁵, Reto Knutti^{6,1}, and Jean Francois Lamarque¹

¹National Center for Atmospheric Research, Boulder, CO, USA

²Department of Atmospheric Sciences, Texas A&M University, College Station, TX, USA

³Lawrence Berkeley National Lab, CA, USA

⁴Department of Atmospheric and Oceanic Sciences and Institute of Arctic and Alpine Research, University of Colorado, Boulder, CO, USA

⁵School of Atmospheric Sciences, Sun Yat-sen University, Guangzhou, China

⁶Institute for Atmospheric and Climate Science, ETH, Zurich, Switzerland

Correspondence to: Benjamin Sanderson (bsander@ucar.edu)

Abstract. The Paris Agreement of December 2015 stated a goal to pursue efforts to keep global temperatures below 1.5°C above pre-industrial levels and well below 2°C. The IPCC was charged with assessing climate impacts at these temperature levels, but fully coupled equilibrium climate simulations do not currently exist to inform such assessments. In this study, we produce a set of scenarios using a simple model designed to achieve long term 1.5°C and 2°C temperatures in a stable climate. These scenarios are then used to produce century scale ensemble simulations using the Community Earth System Model, providing impact-relevant long term climate data for stabilization pathways at 1.5°C and 2°C levels and an overshoot 1.5°C case, which are freely available to the community. Here we describe the design of the simulations and key aspects of their impact-relevant climate response. Exceedance of historical record temperature occurs with 60 percent greater frequency in the 2°C climate than in a 1.5°C climate aggregated globally, and with twice the frequency in equatorial and arid regions. Extreme precipitation intensity is statistically significantly higher in a 2.0°C climate than a 1.5°C climate in several regions. The model exhibits large differences in the Arctic which is ice-free with a frequency of 1 in 3 years in the 2.0°C scenario, and only 1 in 40 years in the 1.5°C scenario.

1 Introduction

The Paris Agreement of 2015 changed the landscape of climate negotiations by framing the debate on future policy in terms of temperature targets which would require substantial globally coherent emissions reductions in the near future (Sanderson et al., 2016). Mitigation efforts required to achieve a likely probability of staying below the upper limit (2°C) exceed those combined efforts currently pledged by the countries (Rogelj et al., 2016). The Representative Concentration Pathways (RCPs) for the Coupled Model Intercomparison Project (CMIP) which informed the 5th Assessment Report of the IPCC (AR5, Pachauri et al. 2014) diverged in 2005. Since then, the world's emissions have been closer to the highest emissions pathway (RCP8.5) than



any other, even accounting for a recent slowdown in emissions growth (Van Vuuren et al., 2011; Quéré et al., 2016). Current policy (if enacted) would result in a middle-of-the-road emissions pathway resulting in a 2.5-4°C warming level (Kitous and Keramidas, 2015). For the lower Paris Agreement temperature goal of 1.5°C, coherent efforts beginning in 2017 would require both emissions rate reductions of at least 5% per year (Sanderson et al., 2016) and a commitment to negative emissions levels which would lie on the verge of economic and physical plausibility (Smith et al., 2016).

Aside from the feasibility or costs of any scenario, it is important to quantify in which ways a climate of 1.5°C above pre-industrial would be different from 2°C, for others to assess whether avoided impacts could justify the costs of the more stringent mitigation. The study of a 1.5°C world, however, is complicated by a number of factors. The lower temperature goal of 1.5°C exhibits less warming than would likely be achieved in the most aggressive mitigation Representative Concentration Pathway (RCP2.6) considered in the 5th Assessment Report of the IPCC (Van Vuuren et al., 2011). Although some individual models exhibited less than 1.5°C warming in this scenario, there is no comprehensive dataset of Earth System Model (ESM) simulations at this mitigation level. Furthermore, no individual model has performed a large ensemble of RCP2.6 which fully samples internal variability at a low forcing level.

Second, the RCP2.6 scenario diverged from historical emissions pathways in 2005, and the lack of significant global mitigation action since that point means that future mitigation action required to achieve 1.5°C are now radically different from what would have been necessary in 2005 (Sanderson et al., 2016; Stocker, 2013). As such, the transient climate evolution of RCP2.6 could noticeably differ from a 2.0°C scenario where mitigation action begins in 2017.

Numerous strategies have been proposed for addressing this discrepancy of scenarios. Pattern scaling techniques, which assume that patterns of temperature and precipitation change can be scaled by global mean temperatures or by finding time periods from other scenarios where the global mean temperature is equivalent to the target level, can produce quite skillful reproductions of mean climate shifts (Tebaldi and Arblaster, 2014). However, climate impacts are often functions of the extremes of the distribution, which may not scale in a simple fashion with global mean temperature, especially for precipitation (Pendergrass and Hartmann, 2014). Another approach is to ‘time-shift’, by taking periods in existing simulations where global mean temperatures equal the warming level of interest. Schleussner et al. (2016) used this approach to compare impacts at 1.5°C and 2°C. However, time-shifting approaches can be complicated when using a period of transient change still exhibiting a strong trend, because the pattern of warming may differ from the equilibrium state (Herger et al., 2015).

An international modelling effort, "Half a degree Additional warming, Projections, Prognosis and Impacts" (HAPPI, Mitchell et al. 2017) has been proposed to fill the gap for simulations to inform the planned IPCC special report on 1.5°C. This effort will use prescribed sea surface temperatures (SSTs) which are consistent with a scaled CMIP5-mean estimate of predicted equilibrium 1.5°C and 2.0°C climates. This approach has advantages; it is computationally cheap and rapidly deployable for a large number of modeling groups and can provide a multi-model assessment of impacts at the two temperature levels referred to in the Paris Agreement. However, there are potential limitations to the approach. Because all simulations in HAPPI will have the same SST pattern evolution (with a constant pattern offset to represent warming), the estimate of significance of the difference in climate states will not include any ocean-driven variability. In addition, the use of a single 10 year evolution in



SSTs will produce a narrow sample of modes of internal climate variability, but a comprehensive assessment would require a thorough sampling of coupled ocean-atmosphere variability.

Here we present an ensemble of transient coupled climate simulations with the Community Earth System Model (CESM, version 1 Hurrell et al. 2013) which achieve the 2°C and 1.5°C goals in line with the Paris targets. These simulations provide a test case for conclusions inferred from other methodologies using the same model (such as pattern scaling, or HAPPI). In this paper, we first document a simple climate model emulator which is able to predict the transient evolution of global mean temperature, and using this emulator we produce concentration scenarios which result in stable 2°C and 1.5°C scenarios in CESM for the 21st century, with a third scenario describing a brief overshoot which returns to 1.5°C by 2100. We then assess the broad climatic features of these two scenarios, including how they differ in both mean state and in the frequency of extremes which might relate most strongly to societal impacts. We aim in this study to provide a broad overview of differences in impact-relevant climate variables, while further studies will focus in more detail on specific processes, regions or societal impacts.

2 Methods

2.1 Emulation

The simulations in this study are produced to inform assessment of impacts at 1.5°C or 2°C above pre-industrial levels, and so the end goal is to produce simulations which equilibrate at those temperature targets. Other studies (Sanderson et al., 2016; Meinshausen et al., 2008; Rogelj et al., 2015) have posed the question in terms of devising scenarios which would produce a given temperature target with a certain likelihood (i.e., a certain frequency among a set of GCMs that respond to forcing differently from one another).

But the Paris Agreement requested climate information from IPCC on specific temperature levels: 1.5 and 2°C above pre-industrial levels. In a simple model where variability is limited, this can be achieved by interactively adjusting emissions as a function of past warming (Zickfeld et al., 2009). But in the presence of large internal variability, and in order to produce a GCM simulation which achieves these goals, we need to perform a reverse calibration: to produce an emission scenario which would result in a specific temperature outcome. Because of the computational expense of running a GCM and the natural variability obscuring the forced signal, this inverse problem can alternatively be solved by employing an emulator which can predict the global mean concentration and temperature trajectory for a given emissions scenario, and iteratively adjusting the emissions scenario parameters such that the desired stable temperature level is achieved.

Some simple climate models already exist in the literature, but we chose to design our emulator as a community project, and as such to have it be open-source and publicly available for further community research in line with the climate model and the climate data that we produce. Our main design choice was to minimize the number of its degrees of freedom to allow for fast calibration to reproduce the global mean trajectory of any given GCM. The result is a simple climate model, the Minimal Complexity Earth Simulator (MiCES, 2016) written in MATLAB and capable of emulating the forced global mean temperature and multi-gas concentration evolution of a more complex model with a minimal set of free parameters. The emulator design and calibration process is discussed at length in the supplementary material section A and B, and the code is provided with this



manuscript. For the purposes of this study, the model's parameters were calibrated so that MiCES emulates the Community Earth System Model (version 1.1.1, CESM1-CAM5).

2.2 Scenarios

Once the emulator has been calibrated, we design emissions scenarios which are predicted to produce stable 2°C and 1.5°C climates in CESM1-CAM5 (as in Figure 1(b)). We use the methodology established in Sanderson et al. (2016) to define idealized emissions pathways which produce a smooth emissions trajectory from historical trends into a period of emissions reduction, a net-negative emissions phase (where net-negative emissions are constrained to not exceed levels seen in the SSP database (IIASA, 2016)) and a long-term relaxation to levels compatible with a stable global mean temperature. Scenario parameters are adjusted to produce multi-gas emissions scenarios which achieve 3 outcomes relevant to the 1.5 and 2°C goals:

10 **1.5°C 'never-exceed' (1.5degNE)** This scenario is designed such that expected multi-year global mean temperature never exceed 1.5°C above pre-industrial levels (where pre-industrial is taken as the 1850-1920 mean) in CESM1-CAM5. Emissions follow RCP8.5 until 2017, after which carbon emissions rapidly decline reaching 50 percent of 2017 levels in a decade by 2027. Combined fossil fuel and land use carbon emissions reach net-zero (carbon neutral) in 2038. CO₂ emissions reach a peak net negative level in 2065, with a net flux of -1.8GtC/yr. After this, negative emissions fluxes are reduced, reaching -0.9GtC/yr by 2100 (Figure 1(a)). The magnitude of negative emissions continues to decline throughout the 22nd century, reaching -0.3GtC/yr by 2200 (Figure C1(a)).

15 **1.5°C 'overshoot' (1.5degOS)** This scenario is designed such that expected global mean temperature briefly overshoot before returning to 1.5°C by 2100 in CESM1-CAM5. Emissions follow RCP8.5 until 2017, after which emissions decline slightly less rapidly than in 1.5degNE, such that emissions are halved from 2017 levels by 2032. In this scenario, combined fossil fuel and land use carbon emissions reach net-zero in 2046. The overshoot requires a larger late century negative emissions commitment, with a peak net negative flux of -4.0GtC/yr in 2080. After this, negative emissions fluxes are rapidly reduced, reaching -1.0GtC/yr by 2100, but then remain slightly negative throughout the 22nd century, reaching -0.5GtC/yr by 2200.

25 **2.0°C (2.0degNE)** This scenario is designed such that expected multi-year global mean temperature never exceed 2°C above pre-industrial levels. Emissions follow RCP8.5 until 2017, after which emissions decline significantly less rapidly than in 1.5degNE, such that emissions are halved from 2017 levels by 2042. In this scenario, combined fossil fuel and land use carbon emissions reach net-zero in 2078. The scenario still requires a negative emissions phase but much smaller than the other two scenarios, with a peak net negative flux of -0.8GtC/yr in 2120. After this, negative emissions fluxes are slowly reduced, reaching -0.5GtC/yr by 2200.

30 Using the calibrated MiCES model, the three emissions scenarios are used to produce concentration pathways which can be used in a CESM1-CAM5 simulation. We use CESM1.1.1 with the Community Atmosphere Model (version 5, CAM5) at finite volume 1 degree resolution and the Parallel Ocean Program version 2 at 1 degree resolution, to be consistent with the



previous large ensemble studies using RCP8.5 (Kay et al., 2015) and RCP4.5 (Sanderson et al., 2015). In the low emission scenarios in this paper, only well-mixed greenhouse gas concentration are changed between scenarios, all other forcings (land use, aerosol emissions, and ozone) follow RCP8.5 throughout the 21st century as in (Kay et al., 2015)). A set of 10 simulations are conducted for scenarios *1.5degNE*, and *2.0degNE*, branching from the corresponding historical simulations of Kay et al. (2015) in 2006, running through 2100. A set of 5 simulations are conducted for scenario *1.5degOS*. As such, for each scenario the CESM ensemble samples uncertainty due to internally generated variability conditional on an assumed scenario and model design.

3 Temperature, Sea Level, and Sea Ice

3.1 Global-scale mean changes

Figure 1(b) shows the CESM ensemble mean global mean temperature trajectory for the three scenarios, which broadly shows that the emulation process was able to correctly predict the expected ensemble mean temperature evolution for CESM (compare with Figure C1 in the Supplemental Material). The *1.5degNE* scenario stabilizes in 2050 at 1.5°C above pre-industrial levels and then maintains this temperature until 2100. The *1.5degOS* scenario reaches a peak temperature in 2050 of 1.7° above pre-industrial before cooling to 1.5°C by 2100, and the *2.0degNE* scenario stabilizes at slightly over 2.1°C, reaching 2.1°C by 2090.

We can consider what these global temperature trajectories mean for large scale climate change. Figure 1(c) shows the expected range of possible sea level rise over the 21st century for the three scenarios. The CESM1-CAM5 model can only simulate one component of future sea level rise, that of thermal expansion. Notably it does not include ice sheet melt, so in order to show the range of possible sea level trajectories we use the semi-empirical formulation of Rahmstorf (2007), combined with uncertainty ranges from Horton et al. (2014). The inherent uncertainty in the sea level response at a given emissions level is greater than the difference between the scenarios considered here. Using these estimates, the *1.5degNE* scenario would result in 35–65cm of sea level rise by the end of the century, while the *2.0degNE* scenario would result in 45–75cm of rise. On a longer timescale, these two scenarios will further diverge. Schaeffer et al. (2012) found that by 2300, the most likely estimate from a 1.5°C stable temperature would be a stable 150cm of sea level rise, but a 2°C stable temperature would result in 270cm and still increasing in 2300.

In our simulations, we find one of the most dramatic divergences between the 1.5 and 2°C simulations comes at high latitudes. This is illustrated in Figure 1(d), which shows the annual likelihood of ice-free Arctic September conditions in the three scenarios. Ice-free is defined as a condition where September average Arctic sea ice area is less than 1 million square kilometers. Our analysis counts the number of ice-free September years in a 20 year moving window in each 10 member ensemble to assess the probability of ice-free conditions as a function of time. We find that in *1.5degNE*, ice-free conditions remain rare, a 1 in 40 year occurrence by the end of the century. In *1.5degOS*, the likelihood of ice-free conditions peaks in 2060, where there is a 1 in 15 chance of ice-free conditions - but this likelihood then declines such that the likelihood is similar to *1.5degNE* by 2100. However, the *2.0degNE* shows significantly greater chances of ice-free conditions; by 2100, 1

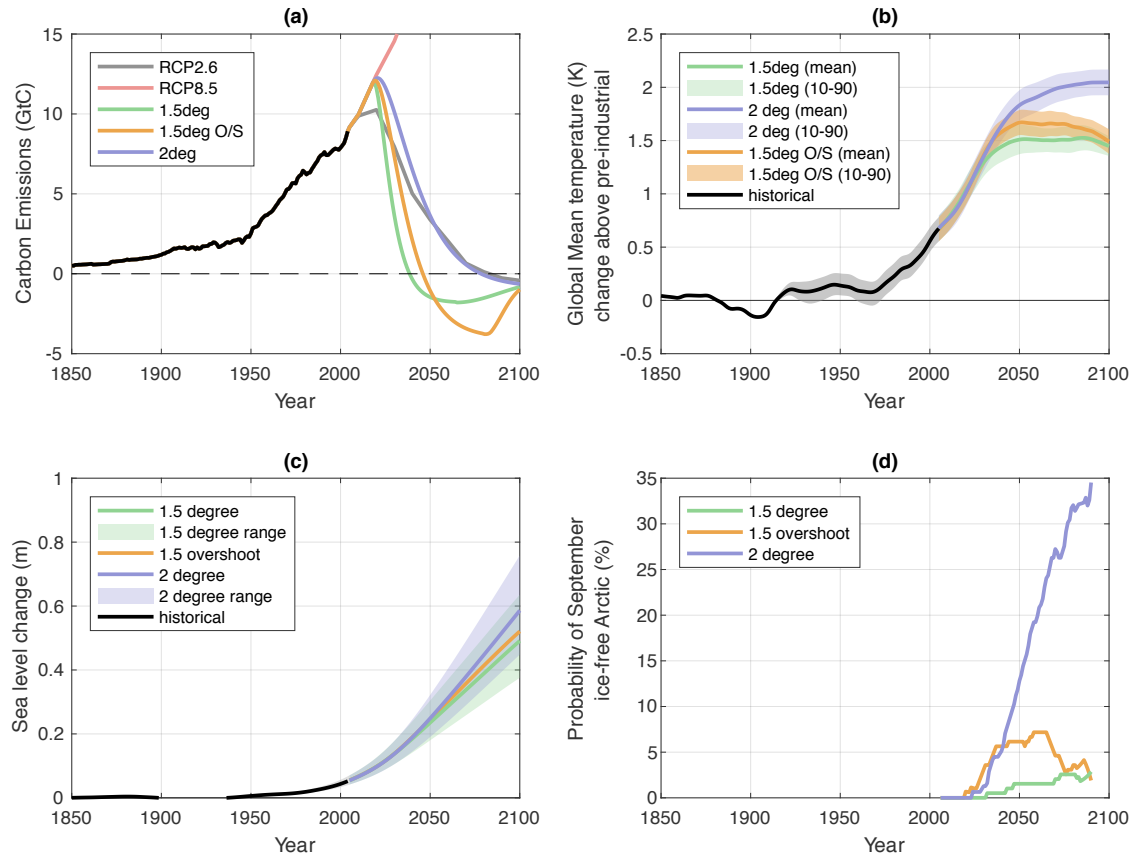


Figure 1. Results from the CESM low emissions scenarios. (a) shows the total carbon emissions trajectory (fossil fuel, cement and land use) used to drive the model simulations. (b) shows the range of annual global mean temperatures changes for the three scenarios, 1.5°C never-exceed (green), 1.5°C overshoot (orange) and 2.0°C (purple). Lines are the most likely values, while the shaded areas are the 10-90 percent expected range in the CESM ensemble. (c) shows the corresponding sea level rise using global mean temperature relationships from Horton et al. (2014) and (d) shows the annual likelihood derived from the CESM ensembles that the Arctic will be ice free in September (20 year running mean).

in 3 years are simulated as ice-free with likelihoods still increasing at the end of the century. It is notable that the difference between the 2.0°C and 1.5°C scenarios largely arises due to the reduced summer survival of multi-year ice in *2.0degNE*, with only 8 percent of annual mean sea-ice in 2100 in *2.0degNE* that is older than one year, compared with 15–20 percent in the *1.5degNE* and *1.5degOS* (and 35 percent in 2005 - see Figure C2 in the Supplemental Material). Compared to recent statistical
 5 analysis of CMIP5 RCP8.5 and RCP4.5 simulations by Screen and Williamson (2017), our results show a higher likelihood of ice-free conditions for *1.5degOS*. The occurrence of ice-free conditions in a 1.5°C world was deemed "exceptionally unlikely"



in Screen and Williamson (2017), but occurs in three out of ten *1.5degOS* ensemble members at least once before the end of the 21st century. All of these occur after the first crossing of the 1.5°C threshold defined by Screen and Williamson (2017), illustrating the importance of dedicated stabilisation simulations for these targets in order to assess the probability of extreme-value climate events such as an ice-free Arctic in the presence of large internal variability. And while it should be noted that Arctic sea ice is lost more rapidly with warming in CESM than in some CMIP5 models (Mahlstein and Knutti, 2012), it is lost less rapidly per degree of global warming than in observations (Rosenblum and Eisenman, 2017).

3.2 Regional Differences

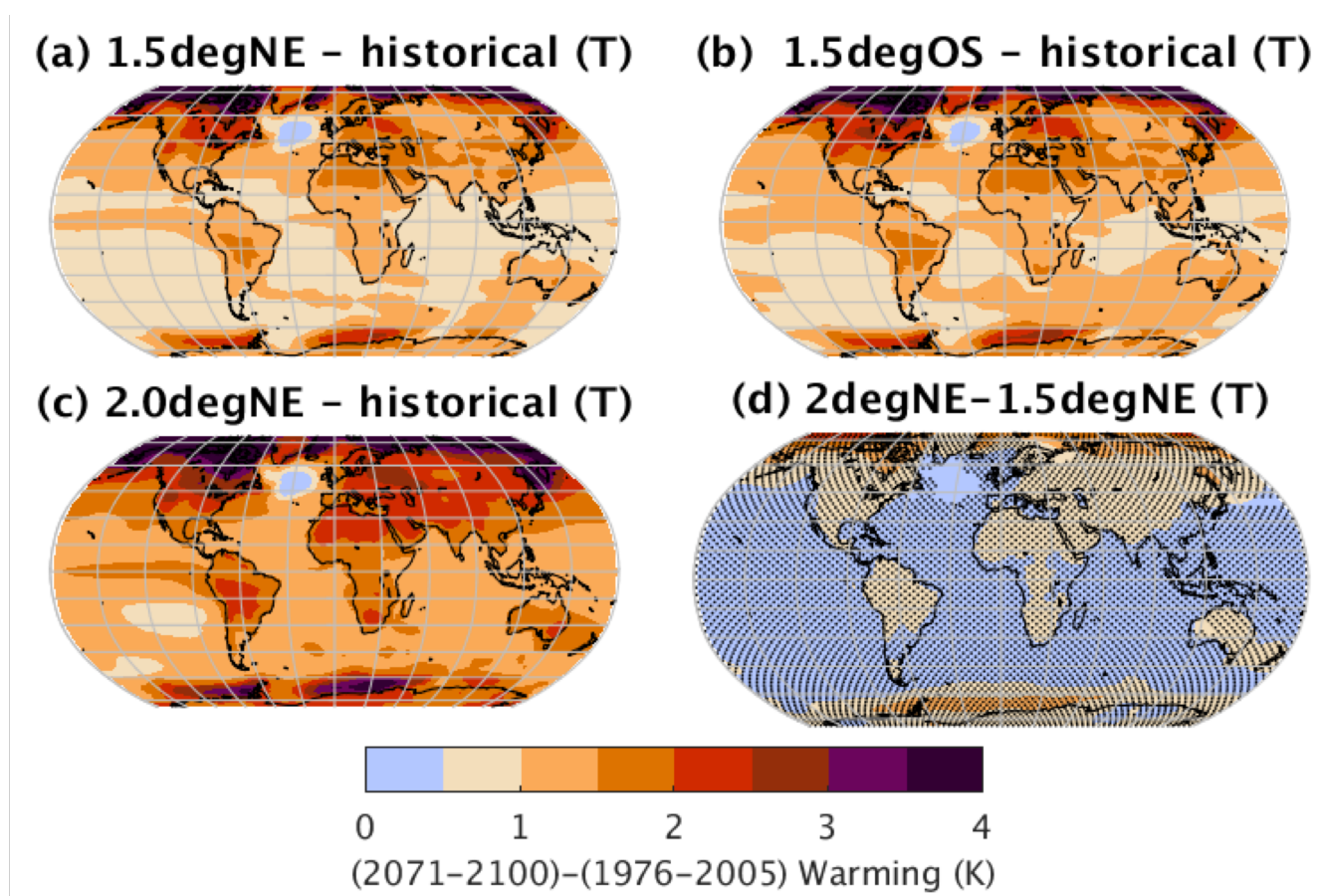


Figure 2. Maps showing ensemble mean 2071-2100 temperature changes relative to 1976-2005 historical conditions in *1.5degNE* (a), *1.5degOS* (b), *2.0degNE* (c) scenarios. Subplots (d) show the difference between mean 2080-2100 conditions in *1.5degNE* and *2.0degNE*, where significant regions are stippled. Significance is defined as a pixel in which the difference between the mean of the *2.0degNE* and *1.5degNE* ensembles exceeds the standard deviation of 2080-2100 values in the *2.0degNE* ensemble.



The regional differences in mean climate between the two scenarios is illustrated in Figure 2. Spatial patterns of warming remain similar in all simulations, with land regions, especially in high latitudes and desert regions, warming more than average. It is notable that for a given global mean temperature target, land temperature warming will be greater: the ensemble mean 2071-2100 land surface temperature is 1.8°C warmer than 1851-1880 in *1.5degNE*, and 2.4°C warmer in *2.0degNE*. At high latitudes, Greenland, for example has an ensemble mean warming of 2.3°C in *1.5degNE* and 3.1°C in *2.0degNE*.

In almost all regions of the globe, the difference in 30 year mean warming for 2071-2100 between *2.0degNE* and *1.5degNE* is statistically significant compared with intra-ensemble random variability (shown in Figure 2(d)). The differences in mean temperature change between *1.5degNE* and *1.5degOS* are subtle, the latter showing more extensive ocean warming and slightly more warming over North America and Central Asia - but most regions do not show detectable differences between the two scenarios at the end of the 21st century (not shown).

3.3 Temperature Extremes

Human impacts such as mortality vary disproportionately with the upper tail of the distribution of temperature (Guo et al., 2014), hence it is of relevance to consider the frequency with which historical temperature extremes will be exceeded in the future. We consider this in a couple of ways, firstly by adapting the methodology of Lehner et al. (2016), which assesses the frequency with which records are exceeded in the future. Figure 3(a) shows the fraction of global land area which is simulated to exceed the observed 1976-2005 record summer temperature in any given year, for each of the three scenarios. By 2040, there is little separation between the scenarios - globally, about 50-60 percent of the global land area exceeds historical temperatures in any given year. However, towards the end of the century, there is a significant difference. 45-55 percent of land area is simulated to exceed the historical record in *1.5degNE*, compared with 70-80 percent in *2.0degNE*. Observations are from Rohde et al. 2013.

Assessed at a regional level, there is greater ensemble spread in the fraction of land area which exceeds the historical record summer temperature (as would be expected from the scale/variability relationships discussed in Deser et al. 2012). However, in the US and in Europe, roughly double the fraction of land experiences historical record breaking summers in *2.0degNE* relative to *1.5degNE* by 2071-2100. Over Asia, the ratio of warming to natural variability is greater for all scenarios, so even the *1.5degNE* scenario is simulated to exceed historical records in 50-90 percent of the region each year (compared with 80-100 percent in *2.0degNE*). It is noteworthy that globally, as well as for the individual regions, the model range encompasses the values derived from observations.

We can consider the spatial distribution of extreme temperature events by following the methodology of Tebaldi and Wehner (2016), which fits a Generalized Extreme Value (GEV) distribution to the upper tail of 3-day temperature averages for both the historical period (1976-2005 in this case) and the future (2071-2100) under different scenarios. The GEV is used to assess, historically, the 3 day average temperature which would be considered a 1 in 20 year event. Figure 5 shows the increase in the expected temperature for a 1 in 20 year 3-day warm event in each of the scenarios. When compared with Figure 2, it becomes clear that some regions experience a greater increase in extreme temperatures than the mean temperature increase. For example, comparing Figure 2(c) and 5(a) - certain regions such as the northern USA/Southern Canada, northern Europe,

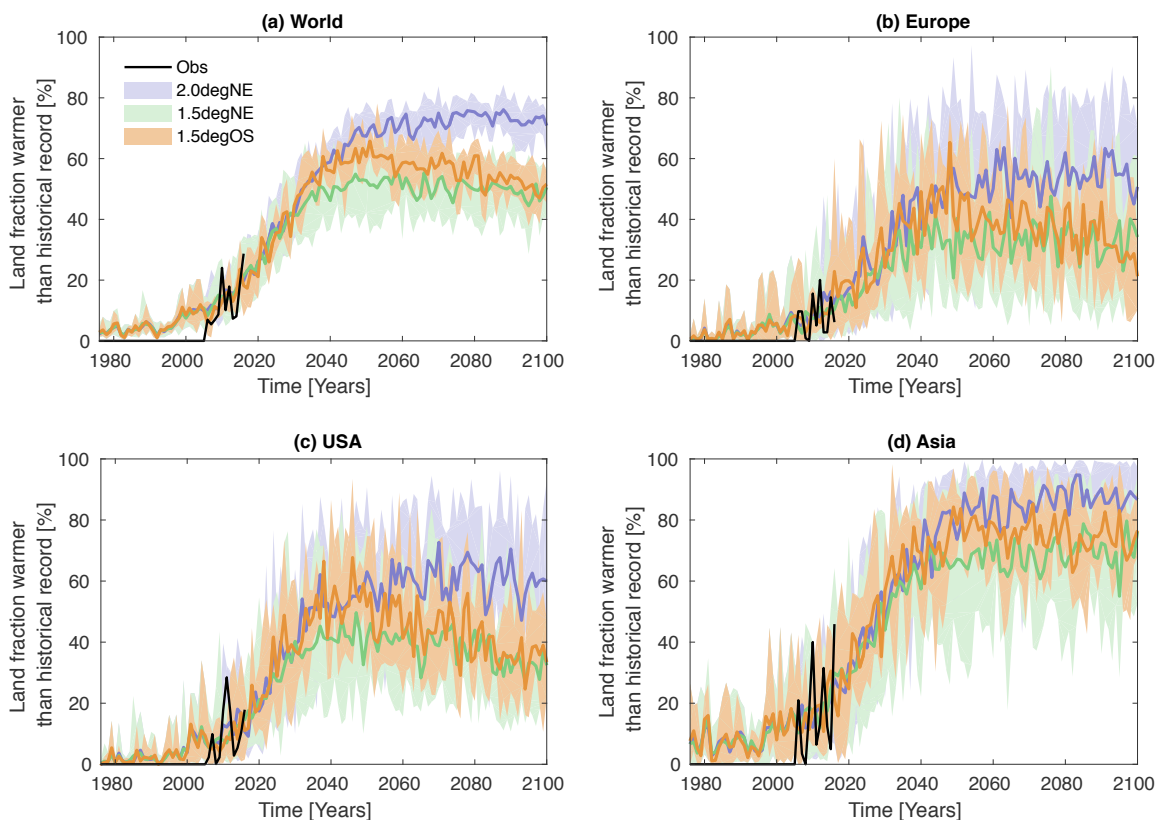


Figure 3. Fraction of land in which the observed historical summer temperature record defined during the period 1976-2005 is broken in any given year. Summer is defined for each grid cell as the climatologically warmest 3-month period. (a) is the fraction of global land area, while (b-d) refer to the fraction of a specific region. The solid central line is the ensemble mean for each scenario, and the shaded areas represent the full ensemble range.

Eastern China and western Brazil/Bolivia which experience increases in extreme 3-day temperatures of about 4K - about twice the mean temperature increase. Comparing *1.5degNE* and *2.0degNE*, most regions globally show a difference of less than 1°C between the scenarios - with the exception of Canada and Northern Europe which show differences of 1-2°C.

We can also consider the expected frequency of exceedence of historical 1 in 20 year 3-day warm event levels. Figure 4 shows the frequency with which these current temperature extremes would be exceeded in *2.0degNE* and *1.5degNE*. This metric shows the greatest increase in regions with a large ratio of mean change to ensemble variability. Because internal variability is greatest at high latitudes in this model (Kay et al., 2015) and indeed in most CMIP5 models (Mahlstein et al., 2011), the greatest signal to noise is seen at lower latitudes. Central Africa, the Saudi Arabian peninsula, Brazil, Peru and to a lesser extent Western India and the Western USA all show significant increases in the frequency of expected exceedance of

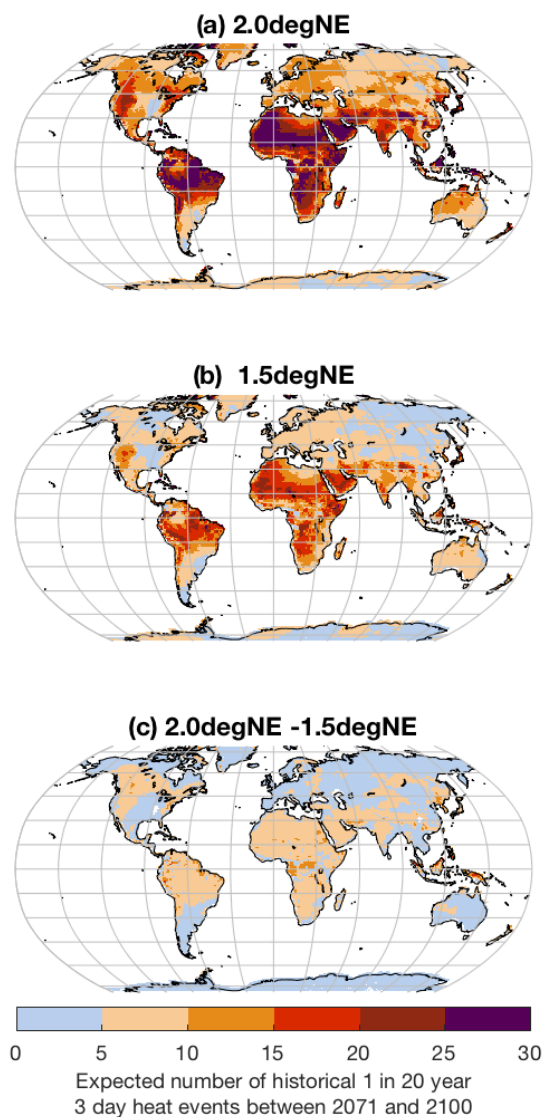


Figure 4. Maps showing the expected number of times that the current 1 in 20 year 3-day warm event would be exceeded during the period 2071-2100 for (a) *1.5degNE*, (b) *2.0degNE* and (c) the difference between the number of events in each scenario. By definition, no change from historical climate would correspond to a value of 1.5 events per 30 years.

the current 1 in 20 year maximum 3-day temperature event. In *1.5degNE*, these regions are simulated to experience 10-20 such events between 2071 and 2100, while in *2.0degNE* exceedance would be an annual event for most of the regions in question.

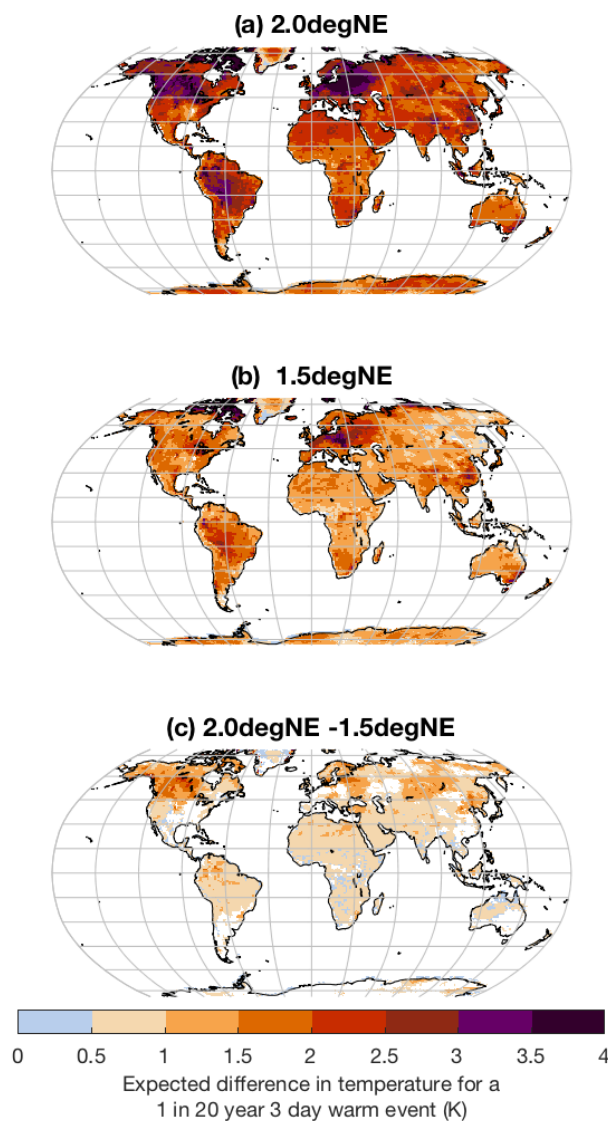


Figure 5. Maps showing the expected difference from 1976-2005 in temperature for a 1 in 20 year 3 day warm event for (a) *1.5degNE*, (b) *2.0degNE* and (c) the difference in temperature between each scenario.

4 Precipitation changes

4.1 Mean

At the global level, there are statistically significant differences in precipitation between 1.5°C and 2°C climates. Global-mean precipitation increases by 3.3 % in *1.5degNE* but 4.5 % in *2.0degNE* from 1976-2005 to 2070-2100 (Figure 6(a); the difference



between the two scenarios exceeds twice the standard deviation of the *2.0degNE*). Over land (Figure 6(b)), mean precipitation increases are slightly less than global mean increases in both cases: 2.8% for *1.5degNE* and 4.3% *2.0degNE* over 1976-2005 levels. At higher latitudes, mean increases are greater at 5.4 and 6.8%. The difference in the mean aggregated land-based precipitation in *1.5degNE* and *2.0degNE* is not significant by the end of the century (neither over all land, nor land north of 5 20°N).

Precipitation differences between the climate states are less significant at the grid point level (Figure 7). All simulations show increased precipitation in the tropics, decreased precipitation in the subtropics and increased precipitation at high latitudes. Very few land regions show a net decrease in precipitation, but there are some exceptions: the southwest US, Amazonia and Indonesia all suggest reductions in precipitation in *2.0degNE*. In most cases, local differences in precipitation between *1.5degNE* and 10 *2.0degNE* are not statistically significant over land; only over the Arctic and Southern oceans are there significant differences (Figure 7(g)).

4.2 Water availability and aridity

Water availability is controlled by joint changes in precipitation minus combined evaporation and transpiration from the surface (hereafter P-E). Figure 7 also shows how P-E changes in the different scenarios. Notably, although very few land regions show 15 a decrease in precipitation, most land regions in all scenarios show a net decrease in P-E by 2071-2100. However, very few regions show a significant difference between changes in *1.5degNE* and *2.0degNE* (exceptions being central Amazonia and the Mediterranean).

We can also consider *aridity*, the ratio of precipitation to potential evapotranspiration (PET, the evaporative demand of the atmosphere; Fu and Feng 2014; Lin et al. 2015). Regions where the ratio of P/PET is less than 0.65 are classified as ‘dry land’ 20 as in Lin et al. (2015). In these simulations, the increase in dry land in a 2°C world is double that of a 1.5°C world: figure 8(a) shows that the global area of dry land increases by 1.25 million km² between 1976-2005 and 2071-2100 under *2.0degNE* while under *1.5degNE*, global aridity peaks in 2040, such that there is an increase of only 0.66 million km² by 2071-2100.

Although the difference in change in total arid area is significant, aggregating changes in aridity by region (Figure 8(b)) suggests that only some regions exhibit statistically significant differences in changes between 2 and 1.5°C climates. Notably 25 both Europe and Southern Africa show large differences in the expected change in aridity by 2071-2100 in *2.0degNE* and *1.5degNE*. Comparing with Figure 7(h), in this is driven largely by Mediterranean regions in Europe and by eastern coast of South Africa and Namibia in Africa.

4.3 Extreme Precipitation

The changing intensity of extreme precipitation is an impact-relevant quantity for ecosystems (Knapp et al., 2008), disease 30 transmission (Curriero et al., 2001) and infrastructure planning (Hossain et al., 2010). We consider the changing patterns of extreme precipitation both at the point level and regionally. Figure 9 shows that only some specific regions would expect large increases in extreme precipitation (quantified here as the annual 1 day maximum rainfall) - eastern Amazonia, Congo, Peru,



central India and northern Canada are simulated to experience a 25-50 percent increase. Differences between the *2.0degNE* and *1.5degNE* are subtle by this metric, with very few regions showing significant differences at the grid point level.

However, when precipitation is aggregated over larger regions, significant differences in extreme behavior between scenarios can become apparent (Fischer and Knutti, 2015). This is illustrated in Figure 10, showing the aggregated relative frequency of events which exceed the historical 99th percentile of daily precipitation. Globally aggregated, there is a large and significant difference between the scenarios: a 7-8 percent increase in events above the historical 99th percentile of daily precipitation in *1.5degNE*, and a 13-15 percent increase in *2.0degNE*. When events are aggregated to the regional level, there are still significant differences in some regions between the frequency of events in *2.0degNE* and *1.5degNE*. High northern latitude regions show consistent separation (Alaska, N.Canada, Greenland, N.Asia), as does the Eastern USA, Eastern Africa, Eastern Asia.

In short, at the grid cell level, there is no significant difference in the likelihood of extreme precipitation events in a 2°C and 1.5°C climate. However, there are significant differences at the regionally and globally aggregated scales.

5 Conclusions and Discussion

In this study, we investigate whether there are significant differences between 1.5°C and 2.0°C of warming in the physical climate system that might have societal impacts. We present a climate model emulator that solves for a concentration pathway leading to a particular temperature target for a particular climate model. Using this emulator, we design three ensembles of coupled climate simulations with a single climate model, CESM, which produce stable equilibrium global mean temperature at 1.5°C and 2°C above pre-industrial levels, the first set of such simulations to our knowledge.

We use these simulations to compare impacts at the two stabilization targets. The question of how substantial this difference in mean climate might be depends on both scale and variable. Mean temperatures are significantly different throughout the globe in a 1.5 and 2°C warmer climate, and various aspects of extreme temperature exposure are distinguishable, especially when aggregated over large areas. We find that 70-80 percent of the global land surface is expected to experience summer temperatures in excess of the pre-2006 record level, every year in the 2°C scenario. Mitigation to 1.5°C reduces this land fraction to 45-55 percent. Exposure to historical 1 in 20 year 3-day heat waves is doubled for most tropical regions in the 2°C world relative to 1.5°C. In central Africa and equatorial South America, this implies that in a 2°C warmer world, historical-period 1 in 20 year 3-day heat waves would be annual events (and approximately biennial for the 1.5°C world). The warmest events also increase disproportionately to the mean in some regions, for example in the USA where mean warming is 1-2°C in a 2°C scenario, but 1 in 20 year 3-day events warm between 2-4°C.

We find also that the difference between 1.5°C and 2°C spans a threshold for the persistence of summer sea-ice in the Arctic, such that ice-free Septembers in the Arctic remain rare in a 1.5°C world, but occur on average every 3 years in a 2°C world. Differences in sea-level rise at these levels is estimated to be on the order of 0.4-0.6m by 2100 in the 1.5°C case, and 0.5-0.75m in the 2°C case, but this 20 percent difference could translate into a higher relative cost impact due to flooding (Brown et al., 2011). However, much of the sea level response occurs on a timescale longer than a century; by 2300 a 2°C



equilibrium climate might be expected to result in almost 3 meters of sea level rise compared with 1.5 meters for a 1.5°C stable climate (Schaeffer et al., 2012).

For mean precipitation, both 1.5°C and 2°C climates show some consistent changes relative to historical levels. Precipitation increases at high latitudes, mountainous regions and western continental boundaries; very few land regions experience a net decrease in precipitation. Increases in evaporation occur globally, such that the net water availability decreases in most regions. Extreme precipitation increases in tropical regions (including western Amazon, Eastern Africa, central India). For both mean and extreme precipitation changes, gridpoint-level differences between a 1.5°C and 2°C climate are not significant over most land areas. But when aggregated regionally, some impact-relevant differences become apparent. Most regions experience an increase in the frequency of events above the historical 99th percentile of precipitation, and this increase is significantly greater in the 2°C simulations than in the 1.5°C simulations - an effect particularly pronounced in high latitude regions. Similarly, although regional changes in aridity are not generally significant, aggregated globally, the increase in dry land is 90 percent greater in the 2°C climate than in the 1.5°C case.

Taken together, it can be argued that if these simulations are representative of the true climate system, there could be substantial differences in impact-relevant aspects of climate, at least regionally, between a climate system stabilized at the 1.5°C and 2°C levels. Further targeted study would be necessary to demonstrate how these differences in climate translate to human and ecosystem impacts. Furthermore, the statements of statistical significance in this study account only for the model's internally variability, and does not account for structural uncertainty. Repeating these experiments with a range of coupled climate models would therefore be of value. The climate model emulator presented here can in principle be applied to other climate models to enable these experiments.

A key factor determining whether or not there are significant differences between 1.5°C and 2°C of warming is the magnitude of the climate system response to a difference of half a degree of warming relative to internal climate variability. The best available tool for investigating this question is ensembles of coupled climate model simulations, because they include the best available estimates of internal climate variability. Simulations with prescribed SSTs exclude internal variability arising from the ocean, or from interactions between the atmosphere and ocean, and yet, the primary tool being pursued by the community to address the difference between 1.5°C and 2°C of warming (HAPPI, Mitchell et al. (2017)) relies on these prescribed-SST simulations. We anticipate that the ensemble of simulations presented here will be a useful benchmark to evaluate the representation of internal climate variability in the HAPPI simulations.

The question of whether a 1.5°C world is 'worth' the mitigation costs beyond the already aggressive goal of 2°C is a complex one, ideally requiring a comprehensive assessment of both the costs and the impacts associated with the two temperature targets. This study focuses on the differences of the physical climate system in order to inform one aspect of this question: are the differences between these temperature targets significant in terms of aspects of climatology which might have societal impacts? To assess the impacts themselves is left for future study, for which we hope these experiments will prove useful.

Our 1.5°C scenarios require net zero emissions by 2040 if the expectation value for global mean temperatures is never allowed to exceed 1.5°C, and by 2045 if a brief overshoot is allowed. These emissions scenarios are conditioned on CESM representing the true climate system, but these dates are broadly consistent with a more general treatment is considered in



Sanderson et al. (2016). However, our model contains no representation of society or economy, and cannot be used to assess the more general question of whether this rate of decarbonization is an achievable goal in reality. Rogelj et al. (2013) considered the probabilistic cost estimates of mitigating to different equilibrium targets, finding that a 1.5°C solution was technically possible in some integrated assessment models with assumptions of low future energy demand. However, a number of studies suggest that the window for a plausible 1.5°C future is rapidly closing, if it has not closed already. Huntingford and Mercado (2016) points out that with many current GCMs, present day concentrations would already result in equilibrium global mean temperatures which would be warmer than 1.5°C. As such, mitigation costs are highly sensitive to political inaction, such that by 2020 in Rogelj et al. (2013), there is no level of carbon taxation which could achieve a 50 percent chance 1.5°C climate.

Mitigation to 1.5°C may or may not be politically feasible. However, it is perhaps more useful to think of a 1.5°C climate as the lowest feasible level of warming which could be achieved this century in ideal conditions: assuming low energy demand, a cooperative global political commitment to decarbonization, fast growth in low carbon technology and development of wide-scale negative emissions infrastructure by mid-century. Simulations such as those presented in this study and those to be conducted in the HAPPI framework provide a quantitative context for the consequences of these idealized conditions failing to be realized. Irrespective of feasibility, these simulations indicate that a relaxation of ambition from the 1.5°C to the 2°C level would result in significantly greater impacts at the global scale, in the tropics and at high latitudes.

6 Code Availability

The simple model used to create and optimize the scenarios used in this study is open-source and freely available at the MiCES github repository (<https://github.com/benmsanderson/mices>).

7 Data Availability

The output data from the simulations produced for this study are freely available at (<http://www.cesm.ucar.edu/experiments/1.5-2.0-targets.html>).

Appendix A: Minimal Complexity Earth Simulator (MiCES)

This study uses a simple model emulator developed by the authors in MATLAB to predict the global mean response of CESM to an emissions scenario, a simple energy balance representation of the Earth's temperature and carbon cycle response. The model

The core of the model is a set of five differential equations. The first describes the evolution of the atmospheric temperature:

$$\frac{\partial T_a}{\partial t}(t) = \frac{1}{\kappa_l} 6.3 \cdot \log(C_a(t)/C_a(0)) + F(t) - \lambda \cdot T_a(t) - D_o \cdot (T_a - T_o) \quad (\text{A1})$$



where t is time, T_a and T_o are the atmospheric and ocean temperatures, $F(t)$ is the sum of all non-CO₂ forcing, κ_l is the thermal heat capacity of the land surface, C_a is the atmospheric carbon content in Pg, λ the climate sensitivity parameter in (K⁻¹) and D_o is the thermal diffusion-like coupling parameter between the atmosphere and the shallow ocean.

The second equation describes the evolution of the atmospheric carbon content:

$$5 \quad \frac{\partial C_a}{\partial t}(t) = \frac{E(t) - (\gamma_l + \gamma_o) \cdot \frac{\partial T_a}{\partial t}(t) \cdot (1 + \delta T_a)}{1 + \alpha(\beta_l)} - \beta_o(\alpha C_a - \rho_o C_o), \quad (\text{A2})$$

where $E(t)$ is the carbon emissions at time t in Pg, γ_l and γ_o are the land and ocean temperature driven carbon feedbacks (in Pg/K), δ is a carbon feedback amplification factor (allowing the carbon release from the land or ocean to respond non-linearly to temperature, in K⁻¹), α is a conversion factor from Pg to atmospheric carbon concentration, β_l is the CO₂ fertilization parameter and β_o is the carbon diffusion coefficient between the atmosphere and ocean, $(\alpha C_a - \rho_o C_o)$ is the difference in
 10 carbon concentration between the atmosphere and ocean, where ρ_o is the conversion factor between ocean carbon content in Pg and ocean carbon concentration.

The third equation describes the evolution of the shallow ocean carbon content:

$$\frac{\partial C_o}{\partial t}(t) = \beta_o(\alpha C_a - \rho_o C_o) + \gamma_o(1 + \delta T_a) \frac{\partial T_a}{\partial t}(t) - \beta_{od} \cdot (\rho_o \cdot C_o - \rho_{od} \cdot C_{od}), \quad (\text{A3})$$

where $\beta_o(\alpha C_a - \rho_o C_o)$ is the diffusion-based carbon flux from the atmosphere, $\gamma_o(1 + \delta T_a) \frac{\partial T_a}{\partial t}(t)$ is the loss of carbon from
 15 the ocean to the atmosphere due to temperature-driven feedbacks, β_{od} is the carbon diffusion coefficient between ocean and deep ocean and $(\rho_o \cdot C_o - \rho_{od} \cdot C_{od})$ is the carbon concentration difference between the shallow and deep oceans (C_{od} is the conversion factor between deep ocean carbon content in Pg and deep ocean carbon concentration).

The fourth equation describes the evolution of carbon in the deep ocean, C_{od} , which changes due a diffusive flux of carbon from the shallow ocean:

$$20 \quad \frac{\partial C_{od}}{\partial t}(t) = \beta_{od}(rho_o \cdot C_o - rho_{od} \cdot C_{od}), \quad (\text{A4})$$

Finally, the fifth equation describes the temperature evolution of the shallow ocean, where κ_o is the thermal heat capacity of the shallow ocean and D_o is the diffusion coefficient. Heat diffusion across the shallow ocean bottom boundary was not found to be a necessary complexity for emulation.

$$\frac{\partial T_o}{\partial t}(t) = D_o \cdot \kappa_o \cdot (T_a - T_o), \quad (\text{A5})$$

25 The source code for MiCES is included in the supplementary material of this paper. Non-CO₂ forcings $F(t)$ are calculated using the atmospheric chemistry model defined and published in Prather et al. (2012), which calculates the lifetimes and radiative forcings of non-CO₂ atmospheric components (CH₄, N₂O, HCFCs, CFCs). Aerosols are calculated by assuming that net aerosol radiative forcing is proportional to global, annual SO_x emissions. The coupled equations are solved using the ODE solver (ode45) in MATLAB.



Appendix B: Tuning for model emulation

The model defined in Section A has a number of free parameters, both in the climate and carbon cycle equations defined in the text and in the chemistry treatment of Prather et al. (2012). Our aim in this study is to reproduce the behavior of the CMIP5 configuration of CESM1-CAM5. (Hurrell et al., 2013). This requires reproducing the carbon-cycle and atmospheric chemistry behavior of the closed-source MAGICC model used to produce the concentration pathways for the RCPs (Meinshausen et al., 2008), as well as emulating the global mean temperature response of CESM1-CAM5.

The free parameters in the model, as well as their prior boundary values, are listed in Table B1.

In order to tune the model to CESM1-CAM5, we perform historical and future climate simulations which can be compared to CESM1-CAM5. Climate simulations are conducted from 1850 to 2100 for the 3 scenarios. The models are validated against CMIP5 simulations from CESM-CAM5. The inputs to MiCES are global total emissions of greenhouse gas emissions (CO_2 , CH_4 , N_2O , CFCs, HCFCs, CO). There is no explicit aerosol scheme in MiCES, instead global mean SO_2 emissions are used as a scaling factor for net anthropogenic aerosol forcing.

The CMIP5 greenhouse gas pathways are derived from MAGICC (Meinshausen et al., 2008), hence our calibration target is actually a hybrid of CESM and MAGICC, where temperatures are matched to CESM and greenhouse gas concentrations to MAGICC's CMIP5 default configuration.

The methane and nitrous oxide components are each calibrated in isolation because their evolution is not sensitive to the temperature or carbon state of the model. In each case, an error function is computed as the sum-squared difference in concentration over the integration period for the 3 scenarios:

$$E^{N_2O}(p) = \sum_{s=1}^3 \sum_{t=1850}^{2100} (c_{mices}^{N_2O}(t, s, p) - c_{magicc}^{N_2O}(t, s))^2 \quad (\text{B1})$$

$$E^{CH_4}(p) = \sum_{s=1}^3 \sum_{t=1850}^{2100} (c_{mices}^{CH_4}(t, s, p) - c_{magicc}^{CH_4}(t, s))^2 \quad (\text{B2})$$

where $E^{N_2O}(p)$ and $E^{CH_4}(p)$ are the error terms for parameter state p , c is the annual mean concentration of methane or nitrous oxide at time t in MiCES and MAGICC, s represents the 3 scenarios (RCP2.6, RCP4.5 and RCP8.5). The parameter state p is initialized from the default values in Prather et al. (2012) and optimized to minimize the value of $E^{CH_4}(p)$ using MATLAB's 'fmincon' function. Other non- CO_2 components (CFCs, HCFCs, CO) are simple decay functions kept at the default values from Prather et al. (2012).

Once the non- CO_2 components are calibrated, the climate component is tuned by considering the temperature from CESM1-CAM5 and the CO_2 trajectories from MAGICC from the CMIP5 RCP2.6, RCP4.5 and RCP8.5 simulations. We start by performing a 10^6 member perturbed ensemble of the model for 3 different scenarios - RCP2.6, RCP4.5 and RCP8.5. Each parameter in the 'climate' sub-component in Table B1 is perturbed using a flat prior sampling with lower and upper bounds as listed. A cost function $E^{climate}(p)$ for the climate components is calculated as a product of combination of the CO_2 and temperature cost functions:



Submodel	Description	Name	Lower	Upper
climate	Climate Sensitivity ($\text{Wm}^{-2}\text{K}^{-1}$)	λ	0.6	3.8
climate	Land Surface Heat Capacity $\text{Ka}^{-1}(\text{Wm}^{-2})^{-1}$	κ_l	1	30
climate	Ocean Heat capacity a^{-1}	D_o	1	300
climate	Atmosphere-ocean diffusion coefficient $\text{Ka}^{-1}(\text{Wm}^{-2})^{-1}$	κ_o	0.001	1
climate	Pre-industrial CO_2 concentration (ppm)	ppm_{1850}	270	290
climate	biosphere CO_2 fertilization parameter (Pg/ppm)	β_l	0	3
climate	biosphere temperature response (Pg/K)	γ_l	-5	0.5
climate	Shallow ocean initial carbon stock (Pg)	$C_o(0)$	100	10000
climate	Ocean carbon diffusion parameter (Pg/ppm)	β_o	0	5
climate	Ocean carbon solubility response (Pg/K)	γ_o	0	0.5
climate	Deep-shallow ocean carbon diffusion coefficient (Pg/ppm)	β_{od}	0.	4
climate	Deep ocean initial carbon stock (Pg)	$C_{od}(0)$	20000	100000
climate	Aerosol 1990 forcing (Wm^{-2})	f_{1990}	-3	0
CH4	Present-day OH feedback, unitless	sOH	-0.37	-0.27
CH4	Present-day loss frequency due to tropospheric CI, 1/a	kCI	0.0025	0.0075
CH4	Present-day loss frequency due to all stratospheric processes, 1/a	kStrat	0.0073	0.02
CH4	Present-day loss frequency due to surface deposition, 1/a	kSurf	4e-3	8e-2
CH4	Present-day loss frequency due to surface deposition, 1/a	cPI	650	750
CH4	Pre-industrial concentration, ppb	cPD	1600	1815
CH4	Present-day growth rate, ppb/a	dcdt	4	6
CH4	Ratio of PI/PD natural emissions, unitless	anPI	0.8	1.2
CH4	Ratio of PI/PD loss frequency due to tropospheric OH, unitless	aPI	0.75	3
CH4	Ratio of y2100/PD loss frequency due to tropospheric OH, unitless	a2100	0.5	2
CH4	Present-day methyl-chloroform decay frequency, 1/a	kMCF	0.176	0.3
CH4	Present-day MCF loss frequency due to ocean uptake, 1/a	kMCFocean	-7.1e-3	7.1e-3
CH4	$k(\text{Species}+\text{OH})/k(\text{MCF}+\text{OH})$ at 272 K	r272	0.1	0.66
N2O	Present-day concentration	cPD	300	326
N2O	Present-day growth rate, ppb/a	dcdt	0.6	0.9
N2O	Pre-industrial concentration, ppb	cPI	100	300
N2O	Present-day loss frequency due to all stratospheric processes, 1/a	kStrat	7.e-3	9e-3
N2O	Ratio of PI/PD loss frequency due to stratosphere, unitless	aPIstrat	0.75	1
N2O	Present-day stratosphere feedback, unitless ($\text{dln}(k\text{Strat})/\text{dln}(C)$)	sStrat	0.06	0.2
N2O	Conversion between tropospheric abundance and total burden, Tg/ppb	b	4.78	4.9
N2O	MCF fill factor, global/troposphere mean mixing ratios, unitless	fill	0.96	1.0
N2O	Ratio of y2100/PD loss frequency due to stratosphere, unitless	a2100strat	0.9	1.1
N2O	Ratio of y2100/PD loss frequency due to tropospheric OH, unitless	a2100	0.9	1.1
N2O	Ratio of PI/PD loss frequency due to tropospheric OH, unitless	aPI	0.5	3.0

Table B1. Parameter Ranges for the MiCES model used in this study.



$$E^{CO_2}(p) = \sum_{s=1}^3 \sum_{t=1850}^{2100} (c_{mices}^{CO_2}(t, s, p) - c_{magicc}^{CO_2}(t, s))^2 \quad (B3)$$

$$E^{T^g}(p) = \sum_{s=1}^3 \sum_{t=1850}^{2100} (T_{mices}^g(t, s, p) - c_{CESM-CAM5}^{T^g}(t, s))^2 \quad (B4)$$

$$E^{climate}(p) = E^{CO_2}(p)E^{T^g}(p), \quad (B5)$$

where c^{CO_2} is the concentration of CO_2 , and T_g is the global mean temperature. The parameter configuration with the lowest cost function in the 10^6 member ensemble is used as an initial condition for an fmincon optimization, which adjusts the parameters to minimize $E^{climate}(p)$. Figure B1 shows the calibrated behavior of MiCES for reproducing the concentrations and temperature response of the CESM1-CAM5/MAGICC hybrid used to create the CMIP5 simulations.

Appendix C: Emissions scenario design

The emissions scenarios developed for this study are not produced in an integrated assessment model. Rather, we use the strategy of Sanderson et al. (2016), which produced idealized emissions scenarios which follow RCP8.5 until a mitigation phase begins at time t_m , after which emissions follow a smooth trajectory (the derivative of emissions is continuous at time t_m), peaking and then decaying asymptotically to an ‘emissions floor’ (E_m^0). A parameter t_m^{50} determines how quickly mitigation occurs, and sets the length of time after t_m that emissions are 50 percent of the way to the asymptotic emissions floor.

In this study, we add a second ‘rampdown’ phase to allow a period of intensive negative emissions followed by a long term relaxation of effort to achieve a stable temperature level. The rampdown phase follows a simple exponential decay, beginning at time t_r , with a long term asymptotic emissions level of E_r^0 and a relaxation time t_r^{50} , such that CO_2 emissions at time t can be described as follows:

$$E(t) = \begin{cases} E_{RCP8.5}, & \text{if } t \leq t_m \\ A_m[(t - t_m^e)e^{-t/\tau_m}] - E_m^0, & \text{if } t_m < t \leq t_r \\ A_r[e^{-(t)/\tau_r}] - E_r^0, & \text{if } t > t_r \end{cases}$$

with 5 parameters to solve: A_m and A_r , t_m^e , τ_m and τ_r . These parameters can be solved using boundary conditions already established. We first solve for the parameters for the mitigation stage by fixing the emissions and rate of change of emissions at time t_m , as well as the timescale of mitigation:

$$E(t_m) = E_{RCP8.5}(t_m) \quad (C1)$$

$$\frac{dE}{dt}(t_m) = \frac{dE_{RCP8.5}}{dt}(t_m) \quad (C2)$$

$$E(t_m + t_m^{50}) = (E_{RCP8.5}(t_m) + E_0)/2. \quad (C3)$$



Scenario	Year to begin mitigation phase	Time to 50% of long term (years, mitigation phase)	Mitigation phase emissions floor (PgC/yr)	Year to begin rampdown phase	Time to 50% of long term (years, rampdown phase)	Long term emissions level (PgC/yr, rampdown phase)
Parameter	t_m	t_m^{50}	E_m^0	t_r	t_r^{50}	E_r^0
1.5 never-exceed	2018	10	-1.8	2065	35	-0.3
2.0 never-exceed	2018	25	-0.85	2120	60	-0.4
1.5 overshoot	2018	18	-4	2080	15	-0.5

Table C1. Parameters for the three scenarios described in this study, using the functional form established in Sanderson et al. (2016), t^m is the year that emissions depart from the RCP8.5 scenario and begin the mitigation phase, t_m^{50} describes the rate of decarbonization in the mitigation phase, defined as the number of years after the mitigation phase start time that the emissions are equidistant between 2018 emissions and the emissions floor level, E_m^0 is the asymptotic level to which carbon emissions decay in the mitigation phase, t_r is the year in which the mitigation phase ends and the rampdown phase begins, t_r^{50} is the number of years after the rampdown start time that the emissions are equidistant between emissions in year E_r^0 and the long term emissions floor level and e_j^r is the asymptotic level to which carbon emissions decay in the rampdown phase.

We can then solve for the rampdown parameters in a similar fashion by fixing the emissions at time t_r to allow a smooth transition into the rampdown phase.

The parameters (E_m^0 , t_m^{50} , t_r , E_r^0 and t_r^{50}) for the three scenarios were adjusted manually to achieve the desired temperature behaviour: a stable 2°C climate, a stable 1.5°C climate and an overshoot of 1.5°C, with a stable 1.5°C climate post-2100. The 5 parameters which were found to achieve these characteristics in the calibrated MiCES model are listed in table C1.

As in Sanderson et al. (2016), non-CO₂ greenhouse gas emissions depart from RCP8.5 at time y_m , and then decay asymptotically in a simple exponential to the RCP2.6 pathway using a timescale defined by t^m . Each follows RCP8.5 until t^m , and then decays to the respective RCP2.6 pathway with the decay constant τ_m , such that for a gas j :

$$E^j(t) = \begin{cases} E_{RCP8.5}^j, & \text{if } t \leq t_m \\ E_{RCP8.5}^j e^{-(t-t_m)/\tau_m} + E_{RCP2.6}^j (1 - e^{-(t-t_m)/\tau_m}), & \text{otherwise} \end{cases}$$

10 Where j can correspond to CH₄, N₂O, CO, VOCs, NO_x, CFC-11, CFC-12, HFC-134a, HCFC-22 and SO_x. There is no separate rampdown phase for non-CO₂ emissions. Non greenhouse gas concentrations (aerosols, ozone etc.) follow RCP8.5 throughout the simulation.

Author contributions. Benjamin Sanderson designed the study and led the analysis and writing, Yangyang Xu and Jean-Francois Lamarque performed CESM simulations, Claudia Tebaldi and Michael Wehner performed extreme temperature analysis, Brian O'Neill provided input



on mitigation literature and conceptual planning, Alexandra Jahn performed sea-ice analysis, Flavio Lehner performed heat records analysis, Angeline Pendergrass participated in precipitation analysis, Warren G. Strand performed data post-processing, Lei Lin performed aridity analysis, Reto Knutti provided conceptual guidance and Jean-Francois Lamarque provided input on the simple model chemistry component.

Acknowledgements.

- 5 . This research was supported by the Regional and Global Climate Modeling Program (RGCM) of the U.S. Department of Energy's, Office of Science (BER), Cooperative Agreement DE-FC02-97ER62402.

Correspondence. Correspondence and requests for materials should be addressed to Benjamin Sanderson. (email: bsander@ucar.edu).



References

- Brown, S., Nicholls, R., Vafeidis, A., Hinkel, J., and Watkiss, P.: The impacts and economic costs of sea-level rise in Europe and the costs and benefits of adaptation. Summary of results from the EC RTD ClimateCost Project, Watkiss, P (editor), 2011.
- Curriero, F. C., Patz, J. A., Rose, J. B., and Lele, S.: The association between extreme precipitation and waterborne disease outbreaks in the United States, 1948–1994, *American journal of public health*, 91, 1194–1199, 2001.
- Deser, C., Phillips, A., Bourdette, V., and Teng, H.: Uncertainty in climate change projections: the role of internal variability, *Climate Dynamics*, 38, 527–546, 2012.
- Fischer, E. M. and Knutti, R.: Anthropogenic contribution to global occurrence of heavy-precipitation and high-temperature extremes, *Nature Climate Change*, 5, 560–564, 2015.
- 10 Fu, Q. and Feng, S.: Responses of terrestrial aridity to global warming, *Journal of Geophysical Research: Atmospheres*, 119, 7863–7875, 2014.
- Giorgi, F. and Mearns, L. O.: Calculation of average, uncertainty range, and reliability of regional climate changes from AOGCM simulations via the “reliability ensemble averaging” (REA) method, *Journal of Climate*, 15, 1141–1158, 2002.
- Guo, Y., Gasparrini, A., Armstrong, B., Li, S., Tawatsupa, B., Tobias, A., Lavigne, E., Coelho, M. d. S. Z. S., Leone, M., Pan, X., et al.: Global variation in the effects of ambient temperature on mortality: a systematic evaluation, *Epidemiology (Cambridge, Mass.)*, 25, 781, 2014.
- 15 Herger, N., Sanderson, B. M., and Knutti, R.: Improved pattern scaling approaches for the use in climate impact studies, *Geophysical Research Letters*, 42, 3486–3494, 2015.
- Horton, B. P., Rahmstorf, S., Engelhart, S. E., and Kemp, A. C.: Expert assessment of sea-level rise by AD 2100 and AD 2300, *Quaternary Science Reviews*, 84, 1–6, 2014.
- 20 Hossain, F., Jeyachandran, I., and Pielke, R.: Dam safety effects due to human alteration of extreme precipitation, *Water resources research*, 46, 2010.
- Huntingford, C. and Mercado, L. M.: High chance that current atmospheric greenhouse concentrations commit to warmings greater than 1.5° C over land, *Scientific Reports*, 6, 2016.
- 25 Hurrell, J. W., Holland, M. M., Gent, P. R., Ghan, S., Kay, J. E., Kushner, P., Lamarque, J.-F., Large, W. G., Lawrence, D., Lindsay, K., et al.: The Community Earth System Model: a framework for collaborative research, *Bulletin of the American Meteorological Society*, 94, 1339–1360, 2013.
- IIASA: SSP Database (Shared Socioeconomic Pathways) - Version 1.1, <https://tntcat.iiasa.ac.at/SspDb/dsd>, 2016.
- Kay, J., Deser, C., Phillips, A., Mai, A., Hannay, C., Strand, G., Arblaster, J., Bates, S., Danabasoglu, G., Edwards, J., et al.: The Community Earth System Model (CESM) large ensemble project: A community resource for studying climate change in the presence of internal climate variability, *Bulletin of the American Meteorological Society*, 96, 1333–1349, 2015.
- 30 Kitous, A. and Keramidas, K.: Analysis of scenarios integrating the INDCs, Joint Research Centre, Sevilla, Spain, p. 11, 2015.
- Knapp, A. K., Beier, C., Briske, D. D., Classen, A. T., Luo, Y., Reichstein, M., Smith, M. D., Smith, S. D., Bell, J. E., Fay, P. A., et al.: Consequences of more extreme precipitation regimes for terrestrial ecosystems, *Bioscience*, 58, 811–821, 2008.
- 35 Lehner, F., Deser, C., and Sanderson, B. M.: Future risk of record-breaking summer temperatures and its mitigation, *Climatic Change*, pp. 1–13, 2016.



- Lin, L., Gettelman, A., Fu, Q., and Xu, Y.: Simulated differences in 21st century aridity due to different scenarios of greenhouse gases and aerosols, *Climatic Change*, pp. 1–16, 2015.
- Mahlstein, I. and Knutti, R.: September Arctic sea ice predicted to disappear near 2 C global warming above present, *Journal of Geophysical Research: Atmospheres*, 117, 2012.
- 5 Mahlstein, I., Knutti, R., Solomon, S., and Portmann, R.: Early onset of significant local warming in low latitude countries, *Environmental Research Letters*, 6, 034 009, 2011.
- Meinshausen, M., Raper, S., and Wigley, T.: Emulating IPCC AR4 atmosphere-ocean and carbon cycle models for projecting global-mean, hemispheric and land/ocean temperatures: MAGICC 6.0, *Atmospheric Chemistry and Physics Discussions*, 8, 6153–6272, 2008.
- MiCES: Minimal Complexity Earth Simulator - github repository, <https://github.com/benmsanderson/mices>, 2016.
- 10 Mitchell, D., AchutaRao, K., Allen, M., Bethke, I., Ciavarella, A., Forster, P., Fuglestedt, J., Gillett, N., Haustein, K., Ingram, W., et al.: Half a degree additional warming, prognosis and projected impacts (HAPPI): background and experimental design, *Geoscientific Model Development*, 2017.
- Pachauri, R. K., Allen, M. R., Barros, V. R., Broome, J., Cramer, W., Christ, R., Church, J. A., Clarke, L., Dahe, Q., Dasgupta, P., et al.: Climate change 2014: synthesis report. Contribution of Working Groups I, II and III to the fifth assessment report of the Intergovernmental Panel on Climate Change, IPCC, 2014.
- 15 Pendergrass, A. G. and Hartmann, D. L.: Changes in the distribution of rain frequency and intensity in response to global warming, *Journal of Climate*, 27, 8372–8383, doi:10.1175/JCLI-D-14-00183.1, 2014.
- Prather, M. J., Holmes, C. D., and Hsu, J.: Reactive greenhouse gas scenarios: Systematic exploration of uncertainties and the role of atmospheric chemistry, *Geophysical Research Letters*, 39, 2012.
- 20 Quéré, C. L., Andrew, R. M., Canadell, J. G., Sitch, S., Korsbakken, J. I., Peters, G. P., Manning, A. C., Boden, T. A., Tans, P. P., Houghton, R. A., et al.: Global Carbon Budget 2016, *Earth System Science Data*, 8, 605–649, 2016.
- Rahmstorf, S.: A semi-empirical approach to projecting future sea-level rise, *Science*, 315, 368–370, 2007.
- Rogelj, J., McCollum, D. L., Reisinger, A., Meinshausen, M., and Riahi, K.: Probabilistic cost estimates for climate change mitigation, *Nature*, 493, 79–83, 2013.
- 25 Rogelj, J., Luderer, G., Pietzcker, R. C., Kriegler, E., Schaeffer, M., Krey, V., and Riahi, K.: Energy system transformations for limiting end-of-century warming to below 1.5 [deg] C, *Nature Climate Change*, 5, 519–527, 2015.
- Rogelj, J., Den Elzen, M., Höhne, N., Fransen, T., Fekete, H., Winkler, H., Schaeffer, R., Sha, F., Riahi, K., and Meinshausen, M.: Paris Agreement climate proposals need a boost to keep warming well below 2 C, *Nature*, 534, 631–639, 2016.
- Rohde, R., Muller, R., Jacobsen, R., Perlmutter, S., Rosenfeld, A., Wurtele, J., Curry, J., Wickhams, C., and Mosher, S.: Berkeley Earth Temperature Averaging Process, *Geoinfor. Geostat.: An Overview 1 : 2*, of, 13, 20–100, 2013.
- 30 Rosenblum, E. and Eisenman, I.: Sea ice trends in climate models only accurate in runs with biased global warming, *J. Climate*, under review, 2017.
- Sanderson, B. M., Oleson, K. W., Strand, W. G., Lehner, F., and O’Neill, B. C.: A new ensemble of GCM simulations to assess avoided impacts in a climate mitigation scenario, *Climatic Change*, pp. 1–16, 2015.
- 35 Sanderson, B. M., O’Neill, B. C., and Tebaldi, C.: What would it take to achieve the Paris temperature targets?, *Geophysical Research Letters*, 43, 7133–7142, 2016.
- Schaeffer, M., Hare, W., Rahmstorf, S., and Vermeer, M.: Long-term sea-level rise implied by 1.5 [deg] C and 2 [deg] C warming levels, *Nature Climate Change*, 2, 867–870, 2012.



- Schleussner, C.-F., Lissner, T. K., Fischer, E. M., Wohland, J., Perrette, M., Golly, A., Rogelj, J., Childers, K., Schewe, J., Frieler, K., et al.: Differential climate impacts for policy-relevant limits to global warming: the case of 1.5° C and 2° C, *Earth System Dynamics*, 7, 327–351, 2016.
- Screen, J. A. and Williamson, D.: Ice-free Arctic at 1.5 [deg]C?, *Nature Clim. Change*, advance online publication, –, <http://dx.doi.org/10.1038/nclimate3248>, 2017.
- 5 Smith, P., Davis, S. J., Creutzig, F., Fuss, S., Minx, J., Gabrielle, B., Kato, E., Jackson, R. B., Cowie, A., Kriegler, E., et al.: Biophysical and economic limits to negative CO₂ emissions, *Nature Climate Change*, 6, 42–50, 2016.
- Stocker, T. F.: The closing door of climate targets, *Science*, 339, 280–282, 2013.
- Tebaldi, C. and Arblaster, J. M.: Pattern scaling: Its strengths and limitations, and an update on the latest model simulations, *Climatic Change*, 10 122, 459–471, 2014.
- Tebaldi, C. and Wehner, M. F.: Benefits of mitigation for future heat extremes under RCP4. 5 compared to RCP8. 5, *Climatic Change*, pp. 1–13, 2016.
- Van Vuuren, D. P., Edmonds, J., Kainuma, M., Riahi, K., Thomson, A., Hibbard, K., Hurtt, G. C., Kram, T., Krey, V., Lamarque, J.-F., et al.: The representative concentration pathways: an overview, *Climatic change*, 109, 5–31, 2011.
- 15 Zickfeld, K., Eby, M., Matthews, H. D., and Weaver, A. J.: Setting cumulative emissions targets to reduce the risk of dangerous climate change, *Proceedings of the National Academy of Sciences*, 106, 16 129–16 134, 2009.

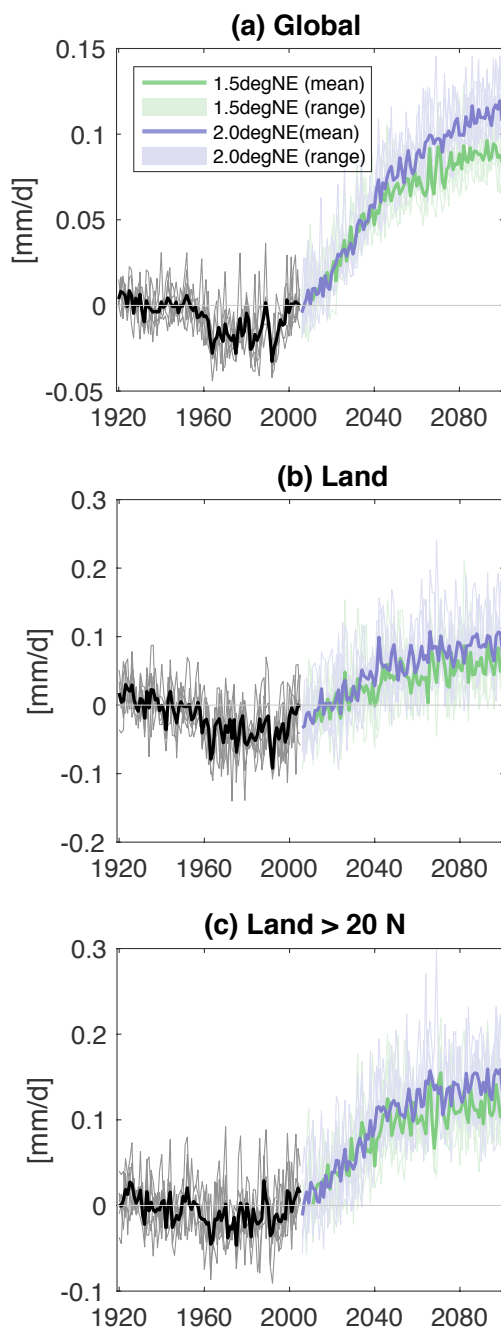


Figure 6. Changes in precipitation at the (a) Global, (b) Land-only and (c) high Northern latitude land. Values are relative to the 1921-1960 average.

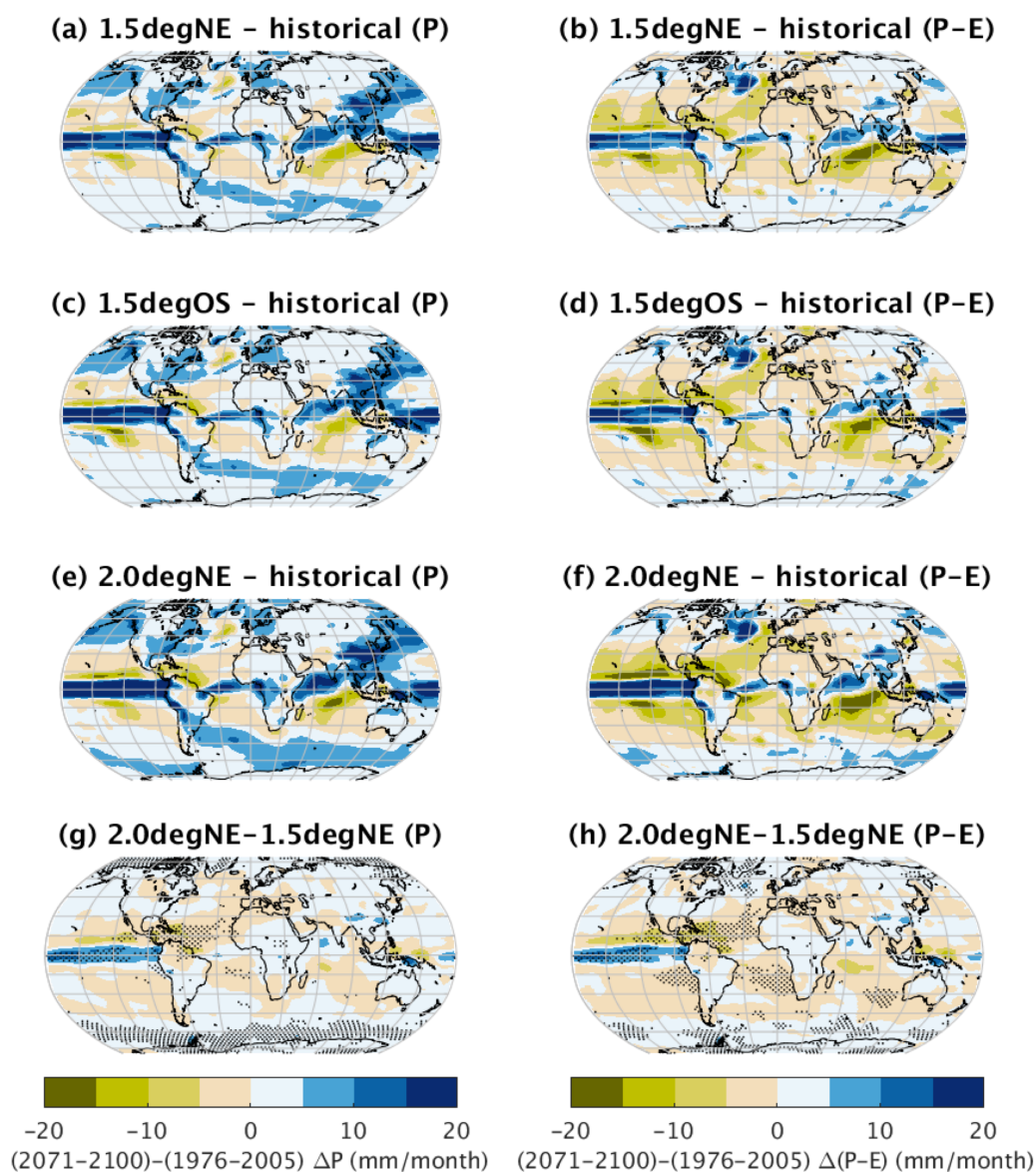


Figure 7. Maps showing ensemble mean 2071-2100 Precipitation and Precipitation-Evaporation changes from 1976-2005 historical conditions in *1.5degNE* (a,b), *1.5degOS* (c,d), *2.0degNE* (e,f) scenarios. Subplots (g,h) show the difference between mean 2080-2100 conditions in *1.5degNE* and *2.0degNE*, where significant regions are stippled. Significance is defined as a pixel in which the difference between the mean of the *2.0degNE* and *1.5degNE* ensembles exceeds the standard deviation of 2080-2100 values in the *2.0degNE* ensemble.

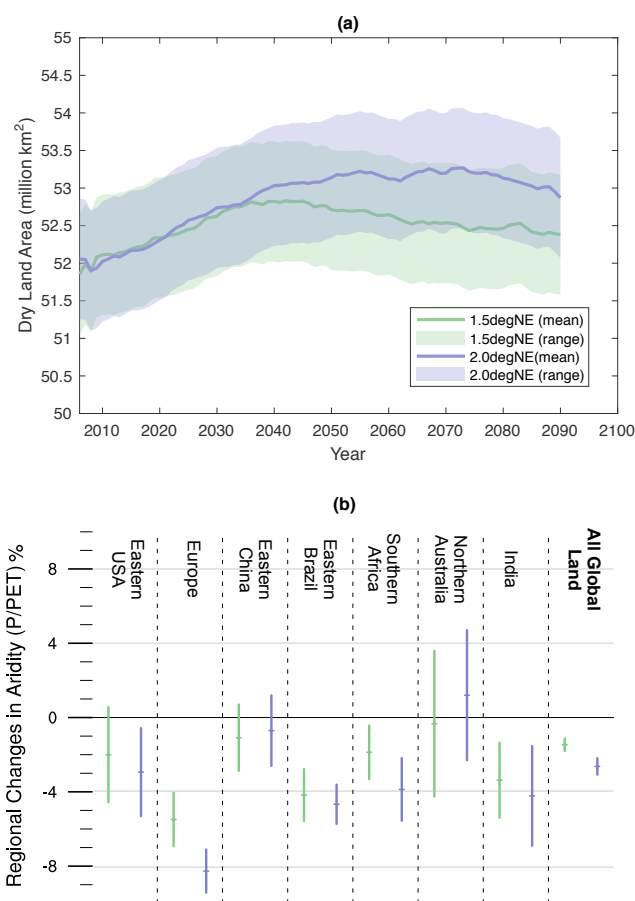


Figure 8. (a) Solid lines show the ensemble mean of aggregated land which qualifies as ‘dry’ land, where aridity (P/PET) <0.65 . Lines are smoothed to show the 20 year running average value. Shaded areas are calculated as ± 1 annual standard deviation from the mean in the respective ensemble. (b) shows the change in aridity for a number of specific regions in 2071-2100 relative to 1976-2005. Central dash indicates the ensemble mean value, while the vertical lines indicate the full spread in the $1.5degNE$ and $2.0degNE$ ensembles.

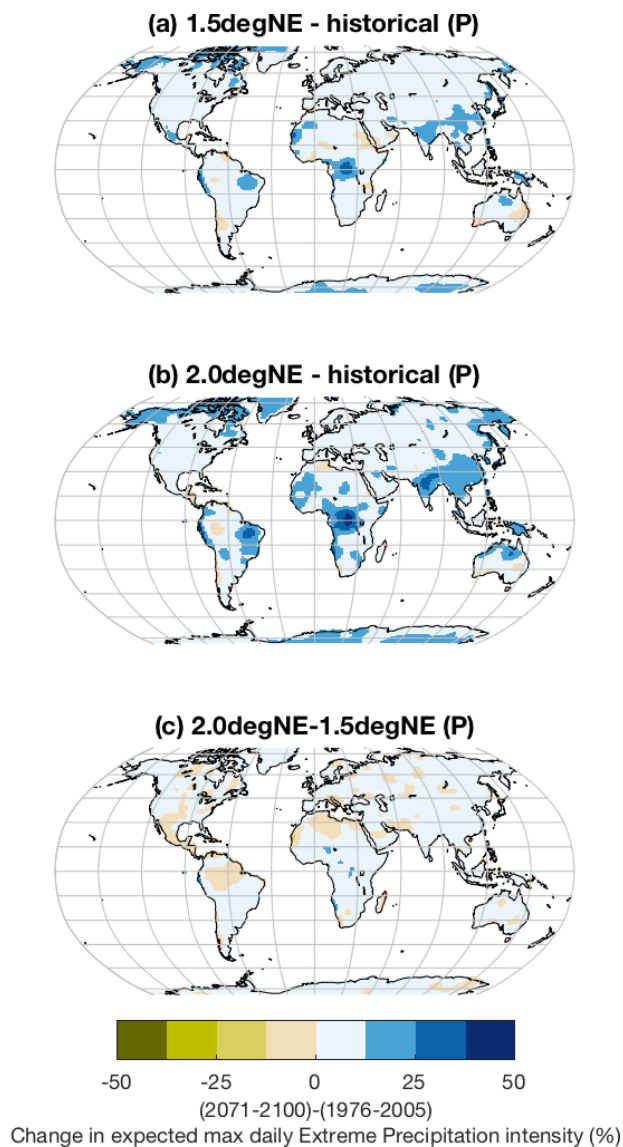


Figure 9. Maps showing the simulated percentage change in ensemble average annual maximum one-day precipitation for historical periods (1976-2005) and future (2071-2100) for (a) 1.5degNE, (b) 2.0degNE and (c) the difference between the scenarios. Maps are smoothed with a 2-D Gaussian smoothing kernel with standard deviation of 2 gridcells.

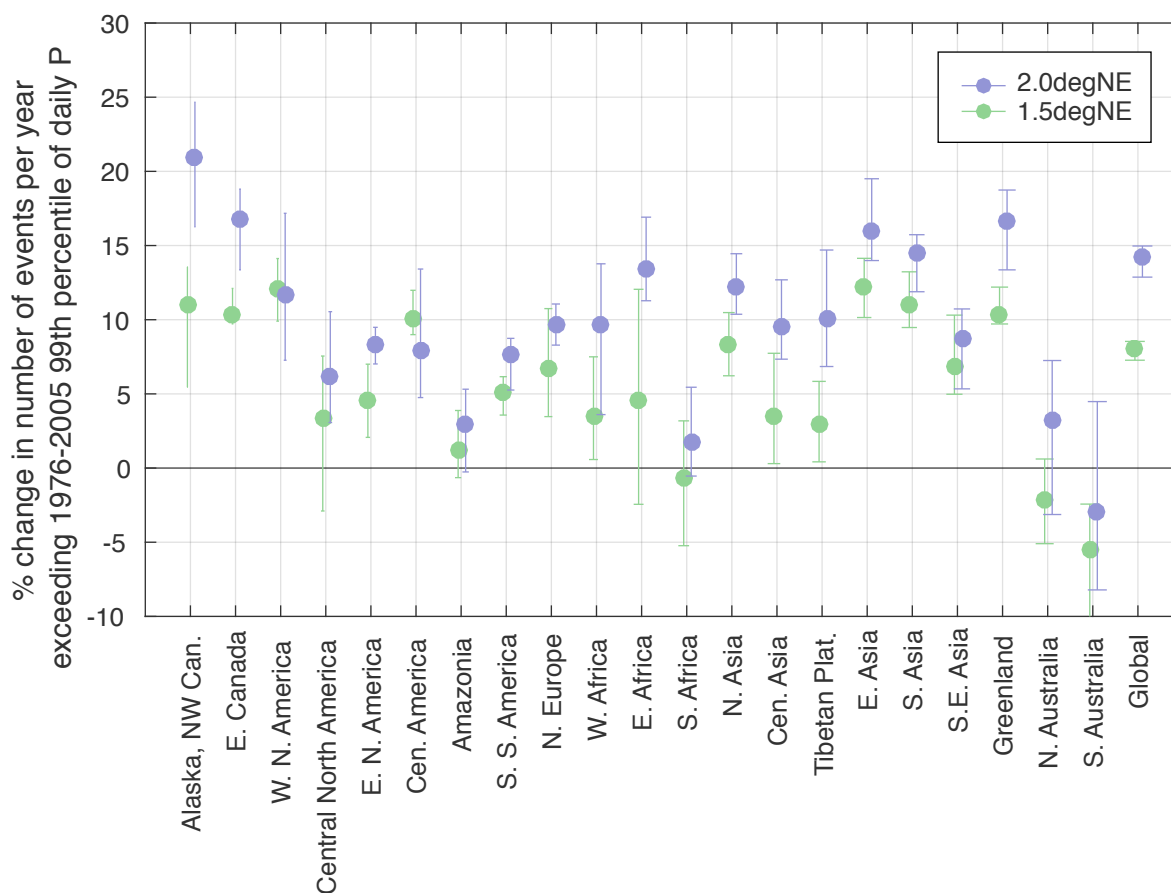


Figure 10. Aggregated percentage change in the aggregated frequency of exceedance of the historical 99th percentile of precipitation over regions as defined in Giorgi and Mearns (2002). Historical 99th percentile is calculated at a grid-cell level from the distribution daily precipitation from years 1976-2005, for ensemble members 1-10 (making 300 years of data). Events exceeding their point-level 99th percentile are summed over the relevant region for each ensemble member, such that the ensemble mean value of the number of exceedances represents the baseline. Future values are calculated from years 2071-2100 of $2.0degNE$ and $1.5degNE$, again summing events which exceed the 1976-2005 99th percentile. The ensemble mean and range of percentage change in number of events in 2071-2100 relative to 1976-2005 is plotted.

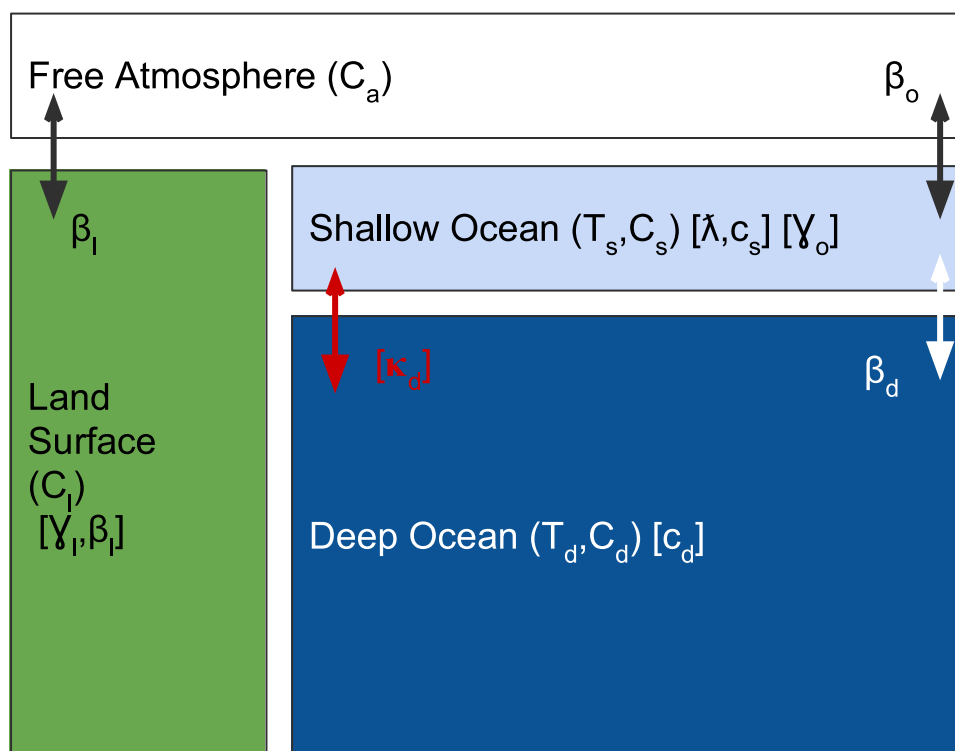


Figure A1. An illustration of the logic flow in the MiCES simple model

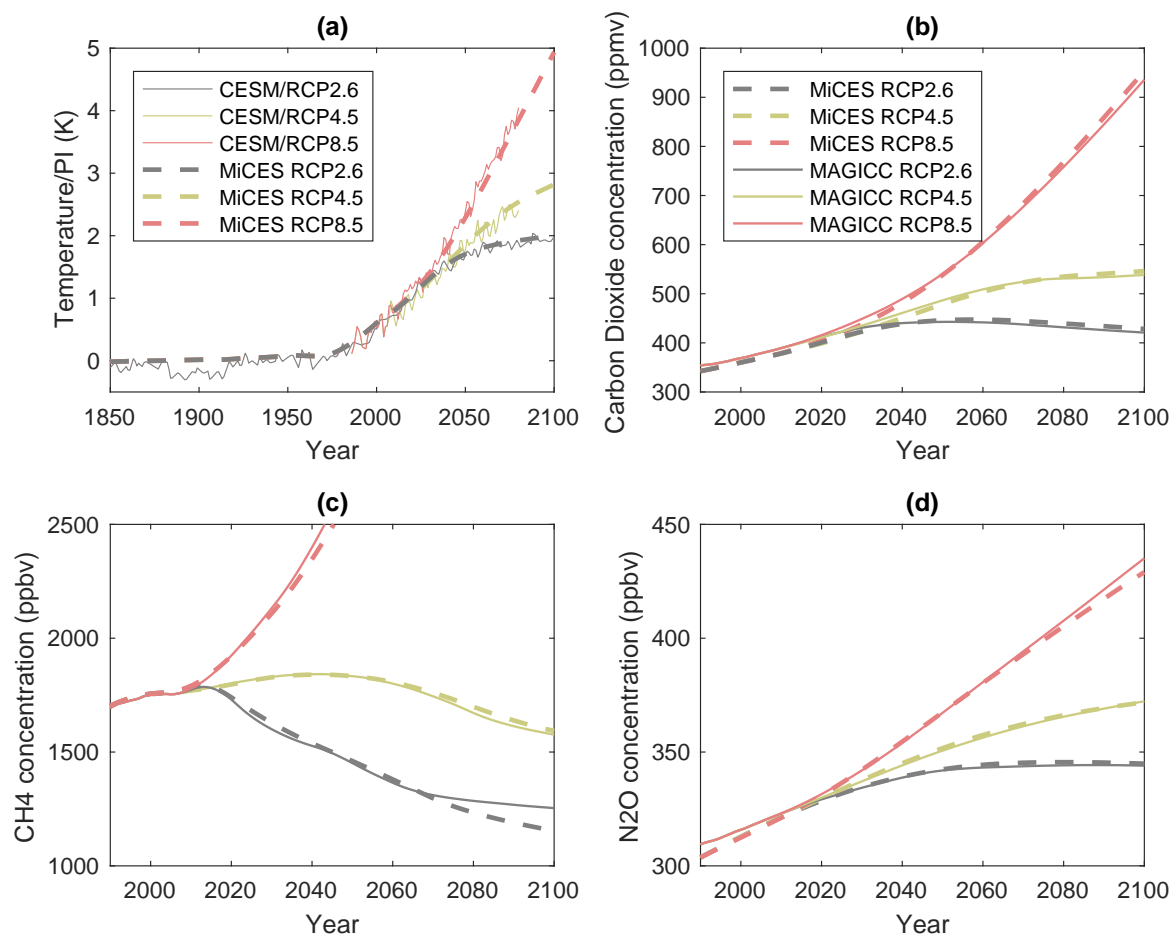


Figure B1. Calibrated behaviour of the MiCES model in the context of the temperature targets (subplot a, target is CESM1-CAM5) and the concentration targets (subplots b-d, where target is MAGICC). In each case, the target is represented by a solid line, and the optimized MiCES simulation is represented by a dashed line. The colors represent the three scenarios used in calibration.

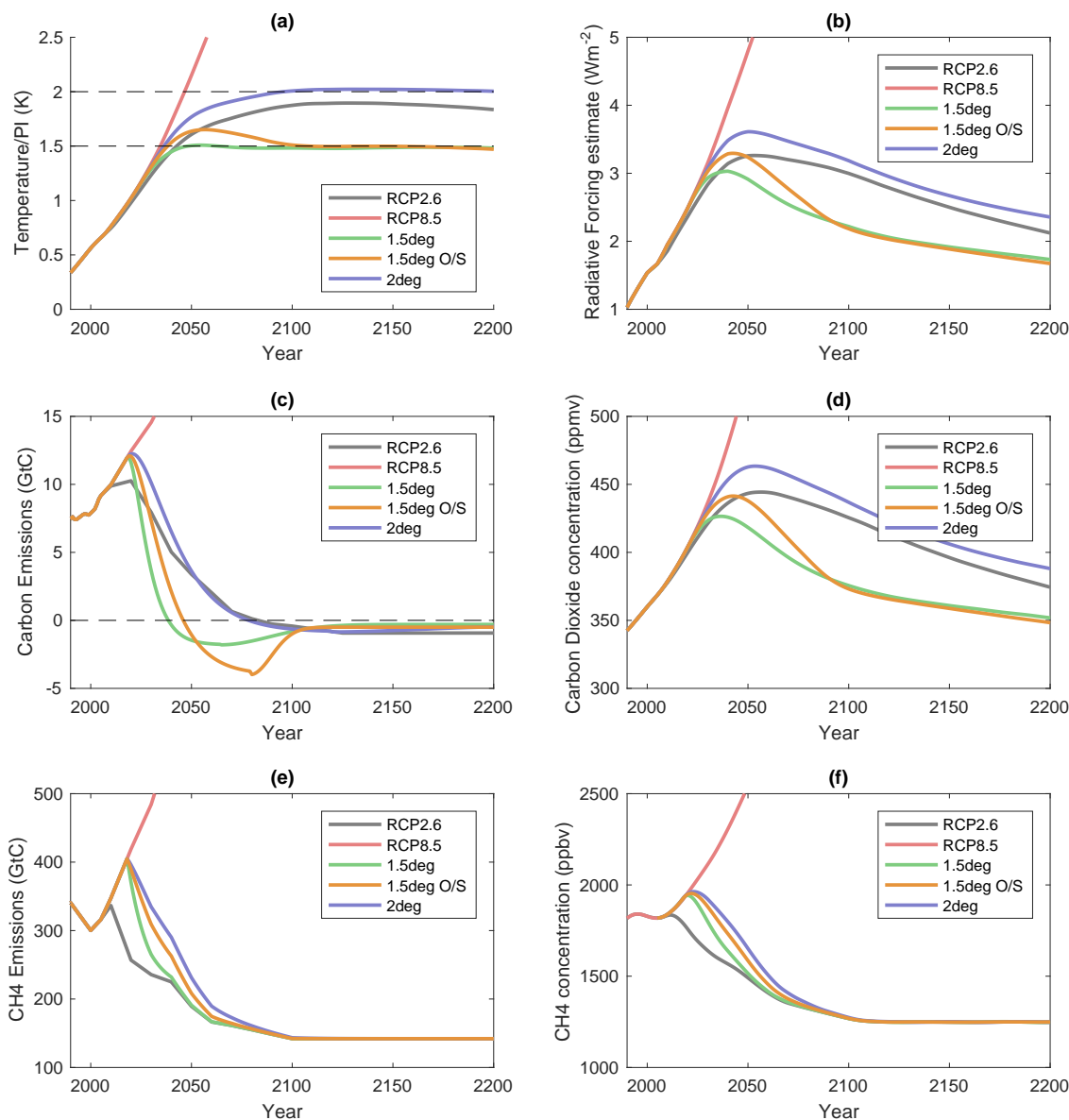


Figure C1. New scenarios used for this study. Figure (a) shows the predicted global mean temperature evolution, (b) shows the radiative forcing evolutions, (c) shows net anthropogenic carbon emissions (fossil fuel and land use combined), (d) shows CO₂ concentrations, (e) shows methane emissions and (f) shows the methane concentrations. Blue, green and orange lines are 2°C, 1.5°C and 1.5°C overshoot respectively.

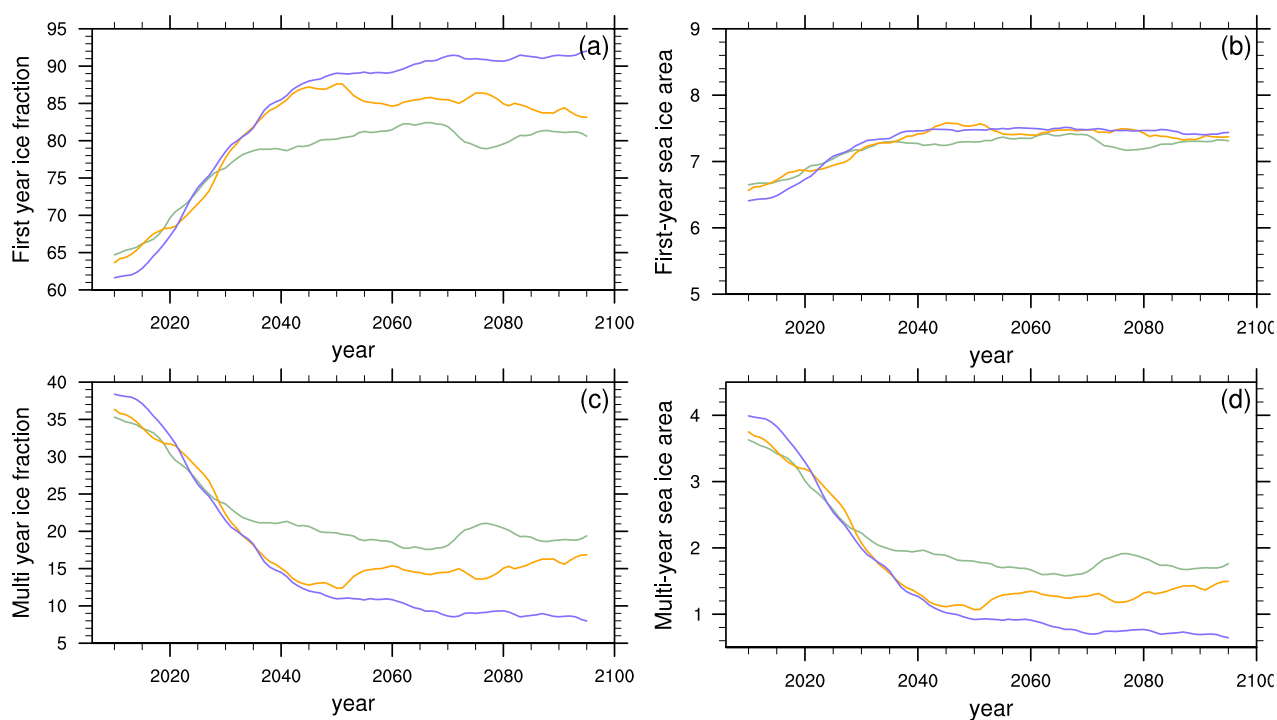


Figure C2. Evolution of the annual 10-year running ensemble-mean of first year and multi-year Arctic sea ice in the low emission simulations. (a) shows the fraction of Arctic sea ice which is less than a year old, (b) shows the sea ice area which is less than a year old, (c) shows the fraction of sea ice which is greater than a year old and (d) shows the total sea ice area which is greater than a year old.